

This is the peer reviewed version of the following article:

Selective changes in inhibition as determinants for limited hyperexcitability in the insular cortex of epileptic rats / A., Bortel; Longo, Daniela; P., De Guzman; F., Dubeau; Biagini, Giuseppe; M., Avoli. - In: EUROPEAN JOURNAL OF NEUROSCIENCE. - ISSN 0953-816X. - STAMPA. - 31:11(2010), pp. 2014-2023. [10.1111/j.1460-9568.2010.07225.x]

Terms of use:

The terms and conditions for the reuse of this version of the manuscript are specified in the publishing policy. For all terms of use and more information see the publisher's website.

08/01/2026 15:36



Published in final edited form as:

Eur J Neurosci. 2010 June ; 31(11): 2014–2023. doi:10.1111/j.1460-9568.2010.07225.x.

Selective changes in inhibition as determinants for limited hyperexcitability in the insular cortex of epileptic rats

Aleksandra Bortel¹, Daniela Longo², Philip de Guzman¹, François Dubeau¹, Giuseppe Biagini², and Massimo Avoli^{1,3}

¹Montreal Neurological Institute and Department of Neurology & Neurosurgery, McGill University, 3801 University, Room 794, Montreal, QC, H3A 2B4, Canada

²Dipartimento di Scienze Biomediche, Università di Modena e Reggio Emilia, Modena, Italy

³Dipartimento di Medicina Sperimentale, Sapienza Università di Roma, Roma, Italy

Abstract

The insular cortex (IC) is involved in the generalization of epileptic discharges in temporal lobe epilepsy (TLE), whereas seizures originating in the IC can mimic the epileptic phenotype seen in some patients with TLE. However, few studies have addressed the changes occurring in the IC in TLE animal models. Here, we analyzed the immunohistochemical and electrophysiological properties of IC networks in non-epileptic control and pilocarpine-treated epileptic rats. Neurons identified with a neuron-specific nuclear protein antibody showed similar counts in the two types of tissue but parvalbumin- and neuropeptide Y-positive interneurons were significantly decreased (parvalbumin, approximately –35%; neuropeptide Y, approximately –38%; $P < 0.01$) in the epileptic IC. Nonadapting neurons were seen more frequently in the epileptic IC during intracellular injection of depolarizing current pulses. In addition, single-shock electrical stimuli elicited network-driven epileptiform responses in 87% of epileptic and 22% of non-epileptic control neurons ($P < 0.01$) but spontaneous postsynaptic potentials had similar amplitude, duration and intervals of occurrence in the two groups. Finally, pharmacologically isolated, GABA_A receptor-mediated inhibitory postsynaptic potentials had more negative reversal potential ($P < 0.01$) and higher peak conductance ($P < 0.05$) in epileptic tissue. These data reveal moderate increased network excitability in the IC of pilocarpine-treated epileptic rats. We propose that this limited degree of hyperexcitability originates from the loss of parvalbumin- and neuropeptide Y-positive interneurons that is compensated by an increased drive for GABA_A receptor-mediated inhibition.

Keywords

interneuron; neuropeptide Y; parvalbumin; pilocarpine; temporal lobe epilepsy

¹Correspondence: Dr Massimo Avoli, Montreal Neurological Institute and Department of Neurology & Neurosurgery, as above. ; Email: massimo.avoli@mcgill.ca.

Introduction

The rat insular cortex (IC) is a heterogeneous cortical area consisting of agranular (localized ventrally), dysgranular and granular (localized dorsally) regions (Shi & Cassell, 1998). The IC is reciprocally connected to several brain regions such as the hippocampus, entorhinal cortex and amygdala (which are all part of the temporal lobe) as well as the thalamus, hypothalamus, parabrachial nucleus and solitary tract nucleus (Allen *et al.*, 1991; Augustine, 1996; Shi & Cassell, 1998). The IC is involved in regulating autonomic responses (Oppenheimer *et al.*, 1991; Butcher & Cechetto, 1995), decoding taste sensations (Cechetto & Saper, 1987; Augustine, 1996; Rosenblum *et al.*, 1997), sensing pain (Jasmin *et al.*, 2003, 2004) and other functions such as ocular movements, memory tasks related to language, auditory processing underlying speech and selective visual attention (Augustine, 1996).

The IC also projects to areas of the frontal motor cortex that are known to generate convulsive seizures (Kelly *et al.*, 2002). Moreover, the IC has been implicated in seizure generation and propagation (Kodama *et al.*, 2001; Mohapel *et al.*, 2001; Guenot & Isnard, 2008), and in pharmaco-resistant temporal lobe epilepsy (TLE) (Isnard *et al.*, 2004). The IC, perirhinal and piriform cortices participate in the propagation of limbic seizures to the frontal cortex and also transmit these discharges to the brainstem and spinal cord (McIntyre & Gilby, 2008).

Structural and functional changes have been identified in the IC of patients with TLE presenting with poor postoperative outcome (Bouilleret *et al.*, 2002; Isnard *et al.*, 2004). In addition, progressive thinning in insular, orbitofrontal and angular regions has been observed in patients affected by pharmaco-resistant TLE (Bernhardt *et al.*, 2009), whereas residual IC after neurosurgery is responsible for causing postoperative seizures in patients with TLE (Cats *et al.*, 2007). Electrical stimulation of the IC produces visceral and somatosensory sensations similar to those observed in some patients with TLE during seizures. Therefore, epileptic discharges originating from the IC could be misdiagnosed as TLE (Isnard *et al.*, 2000, 2004; Ryvlin *et al.*, 2006). Indeed, a retrospective study has shown that seizures specific to the IC can hardly be distinguished from those belonging to the family of the so-called temporal 'plus' epilepsy (Barba *et al.*, 2007) and from those generated in the temporal lobe only. Thus, elucidation of the role of the IC in temporal 'plus' seizures is clinically difficult.

We have recently reported that pilocarpine-treated rats (an established animal model of TLE) (Curia *et al.*, 2008) present with edema in magnetic resonance scans as well as damage represented by loss in glial fibrillary acidic protein immunostaining in astrocytes in brain regions corresponding to the IC and piriform cortex (Biagini *et al.*, 2008). These findings suggested that, in this TLE model, the IC may be involved in status epilepticus (SE)-induced brain damage and presumably in both epileptogenesis and ictogenesis. This evidence therefore led us to investigate some structural and functional changes occurring in the IC of chronically epileptic animals following SE induced by intraperitoneal injection of pilocarpine.

Materials and methods

Animals

Sprague-Dawley rats (Charles River, Montreal, QC, Canada) were housed under controlled environmental conditions at $22 \pm 2^\circ\text{C}$ and with a 12 h light / 12 h dark cycle (lights on from 07:00 to 19:00 h). Animals received food and water *ad libitum*. The experiments were carried out only in adult male rats that were handled in accordance with the principles and guidelines described in the NIH booklet Care and Use of Laboratory Animals (NIH Publications no. 8023, revised 1978). All procedures were approved by the Canadian Council of Animal Care, the Ethical Committee of the University of Modena and Reggio Emilia and the Italian Ministry of Health (authorization no. 100 / 2008-B).

Pilocarpine treatment

Status epilepticus was induced in adult male Sprague-Dawley rats weighing 200–250 g at the time of injection. All efforts were made to minimize the number of animals used. Briefly, rats were injected with a single dose of pilocarpine hydrochloride (380–410 mg / kg, i.p.). To reduce the discomfort caused by peripheral activation of muscarinic receptors, methyl scopolamine (1 mg / kg i.p.) was administered 30 min before the pilocarpine injection. Animal behavior was monitored for approximately 4 h following pilocarpine injection and scored according to Racine's classification (Racine, 1972). Only rats that experienced SE (stages 3–5) for 30 min or more (51.2 ± 2.3 min, $n = 42$; mean \pm SEM) were included in the pilocarpine group. They were used approximately 2 months (8 ± 1 week) after the pilocarpine injection for *in-vitro* electrophysiological studies ($n = 29$ rats) and immunohistochemical analysis ($n = 7$ –14 rats). As reported in previous studies (Cavalheiro *et al.*, 1991; Priel *et al.*, 1996; see for review Curia *et al.*, 2008), all rats experiencing pilocarpine-induced SE later exhibited spontaneous recurrent seizures. Rats (200–250 g) receiving saline injection instead of pilocarpine were used as age-matched non-epileptic control (NEC) animals ($n = 35$ and five rats for electrophysiological and immunohistochemical studies, respectively) and were used for experiments approximately 2 months (8 ± 1 week) after the injection.

Immunohistochemical procedures

Pilocarpine-treated and NEC animals were anesthetized (chloralhydrate, 450 mg / kg i.p.) and perfused via the ascending aorta with 100 mL saline followed by Zamboni fixative (pH 6.9) (Biagini *et al.*, 2005). Brains were postfixed overnight in the same fixative at 4°C and, after cryoprotection by immersion in 15 and 30% sucrose-phosphate buffer solutions, they were frozen and cut horizontally from the ventral side with a freezing microtome (Biagini *et al.*, 2008), obtaining 50- μm -thick horizontal sections at levels -6.38 / -6.60 mm from bregma (Paxinos & Watson, 2007). Changes in neuron-specific nuclear protein (NeuN) immunoreactivity were assessed with a monoclonal antibody (#MAB377; Chemicon, Temecula, CA, USA) (Biagini *et al.*, 2008) used at 1 : 1000 dilution. Interneurons were investigated with a monoclonal antibody against parvalbumin (PV) (#PV25, Swant, Bellinzona, Switzerland; 1 : 5000) (de Guzman *et al.*, 2006) or neuropeptide Y (NPY) (#IHC7180, Peninsula, Belmont, CA, USA; 1 : 500) (Merlo Pich *et al.*, 1992). Endogenous peroxidase was blocked by 0.1% phenylhydrazine in phosphate-buffered saline for 20 min,

followed by several washes in phosphate-buffered saline preceding the incubation with primary antibodies. Immunohistochemistry was performed with the avidin–biotin complex technique and diaminobenzidine as chromogen (cf. Biagini *et al.*, 2008). Secondary antibodies and the avidin–peroxidase complex were purchased from Amersham Italia (Milan, Italy) and diluted 1 : 200 and 1 : 300, respectively. Stained sections were analyzed using the image analysis software KS300 (Zeiss Kontron, Munich, Germany) (cf. Biagini *et al.*, 2005; de Guzman *et al.*, 2006). Background values in NeuN-stained sections were obtained from areas that did not contain any stained cell (i.e. layer I). Stained profiles were discriminated from background throughout the insular region corresponding to the caudal border of the rhinal sulcus (Biagini *et al.*, 1993, 1995). Cell profile counts were determined in each field as the number of positive profiles after transformation in D-circles (i.e. the diameter of circles having the same area as measured) by considering a minimum cutoff value of 2 μm for neuronal nuclei. Neurons that were positive for PV and NPY were manually counted by a collaborator who was unaware of the experimental design. Values obtained for NeuN, PV and NPY counts were transformed by the sampled area in cell densities. Four sections for each animal were investigated and averaged for statistical analysis.

Electrophysiological recordings

Brain slices from NEC and pilocarpine-treated epileptic rats were obtained according to the procedures established by the Canadian Council of Animal Care. Rats were decapitated under isoflurane anesthesia and brains were extracted and placed in cold (1–3°C) oxygenated artificial cerebrospinal fluid. Horizontal brain slices (450 μm thick) including the IC, entorhinal cortex, subiculum and hippocampus proper were cut from –6.10 to –7.10 mm from bregma with a vibratome along the horizontal plane of the brain that was tilted by approximately 10° along a posterosuperior / anteroinferior plane passing between the lateral olfactory tract and the brainstem base (see Fig. 4A). Combined hippocampus / IC slices were transferred to an interface tissue chamber and superfused with oxygenated (95% O₂, 5% CO₂) artificial cerebrospinal fluid at 32–34°C. The artificial cerebrospinal fluid composition was (in mM): 124 NaCl, 2 KCl, 1.25 KH₂PO₄, 2 MgSO₄, 2 CaCl₂, 26 NaHCO₃ and 10 glucose. (RS)-3-(2-Carboxypiperazin-4-yl)-propyl-1-phosphonic acid (10 μM) and 6-cyano-7-nitroquinoxaline-2,3-dione (10 μM) were bath applied. Chemicals were acquired from Tocris Cookson (Ellisville, MO, USA) and Sigma-Aldrich (Oakville, ON, Canada).

The IC intracellular recordings were performed with sharp electrodes filled with 3M K-acetate (Sigma-Aldrich) (tip resistance, 70–100 M Ω) that were connected to an Axoclamp 2A amplifier (Axon Instruments, Union City, CA, USA) with an internal bridge circuit for intracellular current injection. Electrodes were placed in the IC close to the rhinal fissure (Fig. 4A). Resistance compensation was monitored throughout the experiment and adjusted as required. The fundamental electrophysiological parameters of IC cells were measured as follows: (i) resting membrane potential (RMP) after cell withdrawal, (ii) apparent input resistance from the maximum voltage change in response to a hyperpolarizing current pulse (< –0.5 nA), (iii) action potential amplitude, and (iv) action potential duration.

The activation of neuronal networks was performed via a concentric bipolar electrode (Frederick Haer and Co., Bowdoinham, ME, USA) that was positioned in the IC near the recording electrode. In all experiments, the minimum stimulus intensity (duration approximately 100 μ s) that produced a reliable response was selected. Intracellular signals were fed to a computer interface (Digidata 1322A, Axon Instruments) and were acquired and stored using the pClamp 8.0 software (Axon Instruments). Subsequent analysis of these data was performed with the Clampfit 9.2 software (Axon Instruments). Adapting neurons were characterized by the firing rate at the onset of a 2 s duration depolarizing current step that later adapted to a lower rate so that the last interspike interval was at least 50% longer than the first interval. Non-adapting regular firing displayed a discharge pattern with more consistent interspike intervals. Thus, the last interspike interval was not longer than 50% when compared with the first interval. Intrinsic bursting neurons exhibited at least three action potentials that had frequencies larger than 100 Hz, were of decreasing amplitude and rode upon a slow depolarizing envelope.

To estimate the adaptation index, the last interspike interval was divided by the first interval. The reversal potential of stimulus-induced inhibitory postsynaptic potentials (IPSPs) was determined by linear regression from the plot of their amplitude vs. membrane potential. Peak conductance was estimated on the basis of the parallel conductance model reported by Williams *et al.* (1993). In brief, membrane potential values obtained before the stimulation and at the peak of the response were plotted as a function of current intensity. The slopes of these two regression lines were used to estimate the input resistance at rest (R_r) and during the stimulation (R_s) and consequently to define the change in resistance ($R = R_r - R_s$) and peak conductance changes (G) using the following formula: $G = 1 / R$.

Data analysis

Values are expressed as mean \pm SEM and n indicates the number of neurons or slices studied under each specific protocol. The results obtained were compared with the Student's t -test for independent samples, chi-square test or one-way ANOVA followed by Scheffé's test. Regression analysis was used to evaluate data on interevent duration. Results were considered statistically significant if $P < 0.05$.

Results

Immunohistochemical analysis of the insular cortex in pilocarpine-treated rats

We investigated whether neuronal cell loss occurs in the IC region of pilocarpine-treated rats by using an antibody against NeuN. We were unable to observe any obvious change in neuronal cell immunostaining (Fig. 1A and B). Counts of NeuN-positive cell nuclei revealed the presence of comparable values in NEC ($n = 5$) and pilocarpine-treated ($n = 7$) rats ($t_{10} = -0.58$, $P = 0.57$; Fig. 1C). The extension of the sampled cortex was similar in both groups ($t_{10} = 1.61$, $P = 0.14$; Fig. 1D), suggesting that no shrinkage due to lesion was present in pilocarpine-treated rats. Accordingly, cell densities were similar in both groups ($t_{10} = -1.89$, $P = 0.09$; Fig. 1E).

Next, we analyzed any possible change in interneuron subpopulations that were identified with antibodies against PV or NPY (Figs. 2 and 3, respectively). PV-positive interneurons were found to be significantly decreased (-33% ; $t_{17} = 3.91$, $P = 0.00$) throughout all of the IC layers analyzed at level -6.38 from bregma (Fig. 2, compare the control immunostaining in A with pilocarpine-treated rats in B) in pilocarpine-treated as compared with NEC rats (Fig. 2C), whereas the sampled area was similar in both groups ($t_{16} = -0.21$, $P = 0.83$; Fig. 2D). Thus, the respective cell densities (Fig. 2E) were also significantly different (-35% ; $t_{16} = 5.89$, $P = 0.00$).

The NPY-positive interneurons (Fig. 3A and B, showing NPY immunostaining in control and pilocarpine-treated rats, respectively) were also significantly decreased (-34% ; $t_{17} = 2.31$, $P = 0.03$) in pilocarpine-treated rats (Fig. 3C). Comparable areas ($t_{16} = -0.22$, $P = 0.83$) were selected in both NEC and epileptic rats (Fig. 3D). Neuronal cell densities for NPY interneurons were also markedly decreased (-37% ; $t_{16} = 3.34$, $P = 0.00$, Fig. 3E) after pilocarpine treatment. No compensatory changes in the neuropil were noted for NPY interneurons.

Electrophysiological and repetitive firing properties of insular cortex neurons in non-epileptic control and epileptic rats

Analysis of the intrinsic properties of IC neurons recorded intracellularly in NEC ($n = 24$ neurons from 20 slices) and pilocarpine-treated ($n = 25$ neurons from 19 slices) animals revealed no differences in RMP ($t_{47} = -0.26$, $P = 0.79$), action potential amplitude ($t_{47} = 1.21$, $P = 0.23$), action potential duration ($t_{47} = 0.04$, $P = 0.97$) and input resistance ($t_{47} = -1.43$, $P = 0.16$) between the two groups (see Table 1). In addition, two different types of firing were generated by IC neurons recorded in NEC and pilocarpine-treated slices during intracellular injection of depolarizing current pulses (duration, 2 s). The first type was characterized by regular, repetitive firing, whereas the second consisted of an initial burst of action potentials followed by regular firing (Fig. 4B). The proportion of these two firing patterns was similar in NEC (regular firing, $n = 21$; intrinsic bursting, $n = 3$) and pilocarpine-treated (regular firing, $n = 22$; intrinsic bursting, $n = 3$; $t_{47} = 0.05$, $P = 0.96$) tissues (Fig. 4C).

However, 80% of NEC IC neurons ($n = 15$ from 15 slices) presented with adapting regular firing during intracellular injection of depolarizing current pulses (duration, 2 s) and only 20% of them displayed a non-adapting regular firing (Fig. 4B and Da). In contrast, 67% of IC neurons ($n = 15$) recorded from 14 epileptic slices displayed adapting regular firing (Fig. 4B). The adaptation index was 15.1 ± 5.3 and 3.0 ± 0.5 ($t_{28} = 2.11$, $P = 0.04$) for NEC and epileptic neurons, respectively (Fig. 4Da). Linear regression of interevent duration expressed as a percentage of the first measured interval between the spikes in NEC and pilocarpine-treated neurons is shown in Fig. 4Db. The coefficient of determination (r^2) and probability for NEC cells were $r^2 = 0.60$ and $P = 0.00$ and for epileptic neurons $r^2 = 0.21$ and $P = 0.08$, respectively.

Synaptic activity in insular cortex neurons of non-epileptic control and pilocarpine-treated epileptic rats

Spontaneous postsynaptic potentials were recorded at RMP from NEC ($n = 10$ from seven slices, $RMP = -75.9 \pm 1.6$ mV) and pilocarpine-treated ($n = 10$ from nine slices, $RMP = -75.8 \pm 1.5$ mV) neurons (Fig. 5Aa). This type of intracellular activity consisted of depolarizing events that had an amplitude ($t_{18} = 0.59$, $P = 0.56$; Fig. 5Ab), duration ($t_{18} = 0.81$, $P = 0.43$; Fig. 5Ac) and interval of occurrence ($t_{18} = -1.50$, $P = 0.16$; Fig. 5Ad) that were not statistically significant between the two groups. In addition, input / output curves obtained by delivering single-shock stimuli of increasing intensity in the IC showed no differences between NEC ($n = 9$ from seven slices) and pilocarpine-treated ($n = 9$ from seven slices) neurons (Fig. 5B and C). These curves were computed by defining as 100% the current intensity required to evoke depolarizing postsynaptic potentials prior to action potential spiking.

Only four of 18 IC neurons (from 12 NEC slices) responded with action potential bursting after single-shock stimuli delivered within the IC. In contrast, stimulation of pilocarpine-treated slices evoked action potential bursting responses in 14 of 16 neurons (from 14 slices, $t_{32} = 4.87$, $P = 0.00$) (Fig. 6B). As previously reported by Inaba *et al.* (2006) in NEC rat tissue, the stimulus-induced bursting responses recorded at RMP in epileptic IC neurons were characterized by a depolarizing envelope that was superimposed by action potential discharge (Fig. 6A, -73 mV). Injection of steady negative current hyperpolarized the membrane potential, increased the amplitude of the depolarizing envelope and decreased the number of action potentials (Fig. 6A, -83 mV). The opposite was observed during membrane depolarization where neurons responded with decreased amplitude of the depolarizing envelope and increased number of action potentials (Fig. 6A, -61 mV). The duration of these postsynaptic responses after stimulation revealed no difference between NEC (5.3 ± 0.9 s, $n = 4$) and pilocarpine-treated (4.7 ± 0.3 s, $n = 10$; $t_{12} = -0.41$, $P = 0.69$; Fig. 6C) IC neurons. In these experiments we never observed spontaneous bursting events in either NEC or pilocarpine-treated slices.

GABAergic inhibition in non-epileptic control and pilocarpine-treated epileptic insular cortex neurons

Next, we analyzed the reversal potential and peak conductance of the stimulus-induced IPSPs recorded in the two groups of animals in the presence of ionotropic glutamatergic receptor antagonists (i.e. artificial cerebrospinal fluid containing $10 \mu\text{M}$ (RS)-3-(2-carboxypiperazin-4-yl)-propyl-1-phosphonic acid + $10 \mu\text{M}$ 6-cyano-7-nitroquinoxaline-2,3-dione) (Fig. 7). These pharmacologically isolated IPSPs were characterized in NEC and pilocarpine-treated IC neurons recorded at RMP by a monophasic depolarizing component that increased in amplitude during intracellular injection of negative current; in contrast, injection of positive current transformed them into hyperpolarizing potentials (Fig. 7A and B). As illustrated in Fig. 7C, the reversal potential of the IPSPs recorded from pilocarpine-treated IC neurons had a significantly more negative value (-74.9 ± 1.7 mV, $n = 12$ neurons from 10 slices) when compared with the IPSPs generated by NEC IC cells (-64.3 ± 2.7 mV, $n = 9$ from eight slices; $t_{19} = 3.29$, $P = 0.00$). Moreover, the peak conductance associated with this inhibitory component revealed higher values in pilocarpine-treated tissue IC

neurons (113.1 ± 13.7 nS, $n = 12$) than in NEC cells (61.1 ± 12.5 nS, $n = 9$; $t_{19} = -2.73$, $P = 0.01$) (Fig. 7C).

Discussion

The main findings reported in this study can be summarized as follows. First, the IC of pilocarpine-treated epileptic rats is characterized by a significant decrease of presumptive interneurons that were identified with PV and NPY immunohistochemistry, whereas similar values in NeuN-positive cell nuclei were found when NEC and pilocarpine-treated ICs were compared. Second, a larger number of non-adapting principal cells can be identified in the epileptic IC during injection of intracellular depolarizing current pulses. Third, single-shock electrical stimuli could elicit synaptic bursting responses in a larger number of pilocarpine-treated IC neurons than in NEC tissue; however, spontaneously occurring network-driven bursts (such as those reported in the entorhinal cortex or amygdala of pilocarpine-treated rats) (Benini & Avoli, 2006; de Guzman *et al.*, 2008) were never observed. Fourth, the reversal potential of the pharmacologically isolated IPSPs is surprisingly more negative and the associated peak conductance higher in IC neurons recorded intracellularly in pilocarpine-treated animals than in NEC.

Structural and functional changes, such as loss of GABA_A benzodiazepine receptor subtypes and insular hypometabolism, have been reported to occur in the IC of patients with TLE (Bouilleret *et al.*, 2002; Isnard *et al.*, 2004). The insular lobe has also been shown to generate interictal and ictal discharges in the majority of TLE patients analyzed with depth electrodes positioned in this area (Isnard *et al.*, 2004; Guenet & Isnard, 2008). In addition, we have recently reported that, at 24 h after pilocarpine-induced SE, hyperintense signals in magnetic resonance images can be detected from a region corresponding to the IC (Biagini *et al.*, 2008). We also demonstrated in these experiments that astrocytes in the IC are less stained when studied with an antibody against glial fibrillary acidic protein at 72 h after SE (Biagini *et al.*, 2008). It was therefore reasonable to postulate that the IC could play a role in this animal model of TLE and thus to anticipate the presence of significant morphofunctional abnormalities. Contrary to these expectations we did not detect any significant decrease in principal cell density of the IC by using a NeuN antibody. However, we could not firmly establish a loss of presumptive interneurons that were identified by using antibodies for PV and NPY. Hence, these data suggest that the initial pilocarpine-induced SE and / or the successive recurring seizures caused selective damage to these two inhibitory neuron populations. Reduction in inhibitory cells after exposure to SE is common in various limbic areas (Du *et al.*, 1995; Andre *et al.*, 2001; van Vliet *et al.*, 2004; de Guzman *et al.*, 2006, 2008) but it is usually found in the context of a more general pattern of neuronal cell loss.

As reported in other regions of the limbic system (Benini & Avoli, 2006; de Guzman *et al.*, 2006, 2008), NEC and epileptic IC neurons analyzed with sharp electrode intracellular recordings were characterized by similar fundamental electrophysiological properties such as RMP, input resistance and action potential amplitude or duration. In addition, we identified similar proportions of regularly firing and intrinsically bursting cells in the two types of tissue. However, IC neurons recorded in pilocarpine-treated slices demonstrated a higher percentage of non-adapting behavior during injection of depolarizing current pulses

when compared with those recorded from NEC slices. Similar data have been obtained from genetically epilepsy-prone rats by Verma-Ahuja *et al.* (1995), which identified a reduction in spike frequency adaptation. In addition, granule cells in the human epileptic dentate gyrus generate nonadapting, high-frequency firing patterns (Selke *et al.*, 2006). Finally, calcium-activated potassium channels, which are known to contribute to intrinsic firing properties, have been shown to protect against TLE (Brenner *et al.*, 2005).

We have found here that single-shock electrical stimulation delivered in the IC elicits bursting responses in 87% of pilocarpine-treated neurons as compared with 22% of cells tested in NEC slices. These synaptically mediated depolarizations were slow and delayed and presumably reflected a polysynaptic response that could be contributed to by feedforward IPSPs, as reported by Gnatkovsky & de Curtis (2006) in neurons located in the superficial layers of the entorhinal cortex of the isolated guinea pig brain. Both GABA_A and *N*-methyl-D-aspartate receptors play an essential role in the stimulus-induced bursting responses recorded in the IC of NEC rats (Inaba *et al.*, 2006). These bursting responses represent network-driven events sustained by synaptic conductances (Inaba *et al.*, 2006); however, we cannot exclude that the changes in firing adaptation and / or the decrease in interneuron subpopulations (both discussed above) could contribute to the higher propensity of pilocarpine-treated IC neurons to generate stimulus-induced epileptiform responses. However, the impact of this structural change on the function of the surviving inhibitory cells as well as on the responses of principal neurons to GABA release is challenged by the surprising data identified by studying the pharmacologically isolated IPSPs. Indeed, in the presence of ionotropic glutamatergic receptor antagonists we found a shift of the IPSP reversal potential to a more hyperpolarized value in pilocarpine-treated IC neurons as compared with NEC cells.

The increased hyperpolarizing drive seen in epileptic IC neurons may represent a compensatory mechanism to the reduced number of interneurons. Previous studies have shown that the potassium-chloride cotransporter 2 (which regulates the reversal potential of GABA_A receptor-mediated responses) is downregulated in animal models of epilepsy (Jin *et al.*, 2005; Pathak *et al.*, 2007; Blaesse *et al.*, 2009) and in human epileptic tissue (Huberfeld *et al.*, 2007). We also found that the alteration of the IPSP reversal potential in neurons recorded in the epileptic IC was associated with a significant increase in the IPSP-mediated peak conductance.

In conclusion, our study reveals a significant decrease of interneurons in the IC of pilocarpine-treated epileptic animals without any concomitant change in principal cell counting. In addition, our electrophysiological analysis demonstrates that, in spite of a higher proportion of stimulus-induced bursting discharges, subthreshold synaptic responsiveness and spontaneously occurring postsynaptic potentials have similar characteristics in the two types of tissue. Hence, IC networks appear to be less prone to generate paroxysmal discharges in the *in-vitro* slice preparation. Indeed, we are inclined to interpret such a 'mild epileptic hyperexcitability' as the result of a surprising shift in the negative direction of the reversal potential of pharmacologically isolated IPSPs (as well as the increased peak conductance). The IC is definitely substantially preserved in pilocarpine-treated animals and it is probably not critical to seizure generation. However, our findings do

not exclude that the IC could be actively involved in seizure generalization, as found in patients with TLE.

Acknowledgments

This study was supported by the Canadian Institutes of Health Research (Grant MOP-8109), Collaborative Health Research Projects (CHRPJ 323272-06), Mariani Foundation (Grant R-06-50), Emilia-Romagna Region (Region-University Program 2007 / 09, Grant 1232) and Savoy Foundation. We thank Ms Toulia Papadopoulos for editorial assistance.

Abbreviations

IC	insular cortex
IPSP	inhibitory postsynaptic potential
NEC	non-epileptic control
NeuN	neuron-specific nuclear protein
NPY	neuropeptide Y
PV	parvalbumin
RMP	resting membrane potential
SE	status epilepticus
TLE	temporal lobe epilepsy

References

- Allen GV, Saper CB, Hurley KM, Cechetto DF. Organization of visceral and limbic connections in the insular cortex of the rat. *J Comp Neurol*. 1991; 311:1–16. [PubMed: 1719041]
- André V, Marescaux C, Nehlig A, Fritschy JM. Alterations of hippocampal GABAergic system contribute to development of spontaneous recurrent seizures in the rat lithium-pilocarpine model of temporal lobe epilepsy. *Hippocampus*. 2001; 11:452–468. [PubMed: 11530850]
- Augustine JR. Circuitry and functional aspects of the insular lobe in primates including humans. *Brain Res Rev*. 1996; 22:229–244. [PubMed: 8957561]
- Barba C, Barbati G, Minotti L, Hoffmann D, Kahane P. Ictal clinical and scalp-EEG findings differentiating temporal lobe epilepsies from temporal ‘plus’ epilepsies. *Brain*. 2007; 130:1957–1967. [PubMed: 17535836]
- Benini R, Avoli M. Altered inhibition in lateral amygdala networks in a rat model of temporal lobe epilepsy. *J Neurophysiol*. 2006; 95:2143–2154. [PubMed: 16381802]
- Bernhardt BC, Worsley KJ, Kim H, Evans AC, Bernasconi A, Bernasconi N. Longitudinal and cross-sectional analysis of atrophy in pharmacoresistant temporal lobe epilepsy. *Neurology*. 2009; 72:1747–1754. [PubMed: 19246420]
- Biagini G, Merlo Pich E, Carani C, Marrama P, Gustafsson JA, Fuxe K, Agnati LF. Indole-pyruvic acid, a tryptophan ketoanalogue, antagonizes the endocrine but not the behavioral effects of repeated stress in a model of depression. *Biol Psychiatry*. 1993; 33:712–719. [PubMed: 8353166]
- Biagini G, Sala D, Zini I. Diethyldithiocarbamate, a superoxide dismutase inhibitor, counteracts the maturation of ischemic-like lesions caused by endothelin-1 intrastriatal injection. *Neurosci Lett*. 1995; 190:212–216. [PubMed: 7637895]
- Biagini G, D’Arcangelo G, Baldelli E, D’Antuono M, Tancredi V, Avoli M. Impaired activation of CA3 pyramidal neurons in the epileptic hippocampus. *Neuromolecular Med*. 2005; 7:325–342. [PubMed: 16391389]

- Biagini G, Baldelli E, Longo D, Contri MB, Guerrini U, Sironi L, Gelosa P, Zini I, Ragsdale DS, Avoli M. Proepileptic influence of a focal vascular lesion affecting entorhinal cortex-CA3 connections after status epilepticus. *J Neuropathol Exp Neurol*. 2008; 67:687–701. [PubMed: 18596544]
- Blaesse P, Airaksinen MS, Rivera C, Kaila K. Cation-chloride cotransporters and neuronal function. *Neuron*. 2009; 61:820–838. [PubMed: 19323993]
- Bouillieret V, Dupont S, Spelle L, Baulac M, Samson Y, Semah F. Insular cortex involvement in mesiotemporal lobe epilepsy: a positron emission tomography study. *Ann Neurol*. 2002; 51:202–208. [PubMed: 11835376]
- Brenner R, Chen QH, Vilaythong A, Toney GM, Noebels JL, Aldrich RW. BK channel beta4 subunit reduces dentate gyrus excitability and protects against temporal lobe seizures. *Nat Neurosci*. 2005; 8:1752–1759. [PubMed: 16261134]
- Butcher KS, Cechetto DF. Autonomic responses of the insular cortex in hypertensive and normotensive rats. *Am J Physiol*. 1995; 268:214–222.
- Cats EA, Kho KH, Van Nieuwenhuizen O, Van Veelen CW, Gosselaar PH, Van Rijen PC. Seizure freedom after functional hemispherectomy and a possible role for the insular cortex: the Dutch experience. *J Neurosurg*. 2007; 107:275–280. [PubMed: 17941490]
- Cavalheiro EA, Leite JP, Bortolotto ZA, Turski WA, Ikonomidou C, Turski L. Long-term effects of pilocarpine in rats: structural damage of the brain triggers kindling and spontaneous recurrent seizures. *Epilepsia*. 1991; 32:778–782. [PubMed: 1743148]
- Cechetto DF, Saper CB. Evidence for a viscerotopic sensory representation in the cortex and thalamus in the rat. *J Comp Neurol*. 1987; 262:27–45. [PubMed: 2442207]
- Curia G, Longo D, Biagini G, Jones RS, Avoli M. The pilocarpine model of temporal lobe epilepsy. *J Neurosci Methods*. 2008; 172:143–157. [PubMed: 18550176]
- Du F, Eid T, Lothman EW, Köhler C, Schwarcz R. Preferential neuronal loss in layer III of the medial entorhinal cortex in rat models of temporal lobe epilepsy. *J Neurosci*. 1995; 15:6301–6313. [PubMed: 7472396]
- Gnatkovsky V, de Curtis M. Hippocampus-mediated activation of superficial and deep layer neurons in the medial entorhinal cortex of the isolated guinea pig brain. *J Neurosci*. 2006; 26:873–881. [PubMed: 16421307]
- Guenot M, Isnard J. Epilepsy and insula. *Neurochirurgie*. 2008; 54:374–381. [PubMed: 18417157]
- de Guzman P, Inaba Y, Biagini G, Baldelli E, Mollinari C, Merlo D, Avoli M. Subiculum network excitability is increased in a rodent model of temporal lobe epilepsy. *Hippocampus*. 2006; 16:843–860. [PubMed: 16897722]
- de Guzman P, Inaba Y, Baldelli E, de Curtis M, Biagini G, Avoli M. Network hyperexcitability within the deep layers of the pilocarpine-treated rat entorhinal cortex. *J Physiol*. 2008; 586:1867–1883. [PubMed: 18238812]
- Huberfeld G, Wittner L, Clemenceau S, Baulac M, Kaila K, Miles R, Rivera C. Perturbed chloride homeostasis and GABAergic signaling in human temporal lobe epilepsy. *J Neurosci*. 2007; 27:9866–9873. [PubMed: 17855601]
- Inaba Y, de Guzman P, Avoli M. NMDA receptor-mediated transmission contributes to network ‘hyperexcitability’ in the rat insular cortex. *Eur J Neurosci*. 2006; 23:1071–1076. [PubMed: 16519672]
- Isnard J, Guénot M, Ostrowsky K, Sindou M, Mauguère F. The role of the insular cortex in temporal lobe epilepsy. *Ann Neurol*. 2000; 48:614–623. [PubMed: 11026445]
- Isnard J, Guénot M, Sindou M, Mauguère F. Clinical manifestations of insular lobe seizures: a stereo-electroencephalographic study. *Epilepsia*. 2004; 45:1079–1090. [PubMed: 15329073]
- Jasmin L, Rabkin SD, Granato A, Boudah A, Ohara PT. Analgesia and hyperalgesia from GABA-mediated modulation of the cerebral cortex. *Nature*. 2003; 424:316–320. [PubMed: 12867983]
- Jasmin L, Burkey AR, Granato A, Ohara PT. Rostral agranular insular cortex and pain areas of the central nervous system: a tract-tracing study in the rat. *J Comp Neurol*. 2004; 468:425–440. [PubMed: 14681935]
- Jin X, Huguenard JR, Prince DA. Impaired Cl^- extrusion in layer V pyramidal neurons of chronically injured epileptogenic neocortex. *J Neurophysiol*. 2005; 93:2117–2126. [PubMed: 15774713]

- Kelly ME, Staines WA, McIntyre DC. Secondary generalization of hippocampal kindled seizures in rats: examining the role of the piriform cortex. *Brain Res.* 2002; 957:152–161. [PubMed: 12443991]
- Kodama M, Yamada N, Sato K, Sato T, Morimoto K, Kuroda S. The insular but not the perirhinal cortex is involved in the expression of fully-kindled amygdaloid seizures in rats. *Epilepsy Res.* 2001; 46:169–178. [PubMed: 11463518]
- McIntyre DC, Gilby KL. Mapping seizure pathways in the temporal lobe. *Epilepsia.* 2008; 49:23–30. [PubMed: 18304253]
- Merlo Pich E, Messori B, Zoli M, Ferraguti F, Marrama P, Biagini G, Fuxe K, Agnati LF. Feeding and drinking responses to neuropeptide Y injections in the paraventricular hypothalamic nucleus of aged rats. *Brain Res.* 1992; 575:265–271. [PubMed: 1571785]
- Mohapel P, Zhang X, Gillespie GW, Chlan-Fourney J, Hannesson DK, Corley SM, Li XM, Corcoran ME. Kindling of claustrum and insular cortex: comparison to perirhinal cortex in the rat. *Eur J Neurosci.* 2001; 13:1501–1519. [PubMed: 11328345]
- Oppenheimer SM, Wilson JX, Guiraudon C, Cechetto DF. Insular cortex stimulation produces lethal cardiac arrhythmias: a mechanism of sudden death? *Brain Res.* 1991; 550:115–121. [PubMed: 1888988]
- Pathak HR, Weissinger F, Terunuma M, Carlson GC, Hsu FC, Moss SJ, Coulter DA. Disrupted dentate granule cell chloride regulation enhances synaptic excitability during development of temporal lobe epilepsy. *J Neurosci.* 2007; 27:14012–14022. [PubMed: 18094240]
- Paxinos, G.; Watson, C. The rat brain in stereotaxic coordinates. 6. Elsevier Academic Press; New York: 2007.
- Priel MR, dos Santos NF, Cavaleiro EA. Developmental aspects of the pilocarpine model of epilepsy. *Epilepsy Res.* 1996; 26:115–121. [PubMed: 8985693]
- Racine RJ. Modification of seizure activity by electrical stimulation. II Motor seizure. *Electroencephalogr Clin Neurophysiol.* 1972; 32:281–294. [PubMed: 4110397]
- Rosenblum K, Berman DE, Hazvi S, Lamprecht R, Dudai Y. NMDA receptor and the tyrosine phosphorylation of its 2B subunit in taste learning in the rat insular cortex. *J Neurosci.* 1997; 17:5129–5135. [PubMed: 9185550]
- Ryvlin P, Rheims S, Risse G. Nocturnal frontal lobe epilepsy. *Epilepsia.* 2006; 47:83–86. [PubMed: 17105470]
- Selke K, Müller A, Kukley M, Schramm J, Dietrich D. Firing pattern and calbindin-D28k content of human epileptic granule cells. *Brain Res.* 2006; 1120:191–201. [PubMed: 16997289]
- Shi CJ, Cassell MD. Cortical, thalamic, and amygdaloid connections of the anterior and posterior insular cortices. *J Comp Neurol.* 1998; 399:440–468. [PubMed: 9741477]
- Verma-Ahuja S, Evans MS, Pencek TL. Evidence for decreased calcium dependent potassium conductance in hippocampal CA3 neurons of genetically epilepsy-prone rats. *Epilepsy Res.* 1995; 22:137–144. [PubMed: 8777900]
- van Vliet EA, Aronica E, Tolner EA, Lopes da Silva FH, Gorter JA. Progression of temporal lobe epilepsy in the rat is associated with immunocytochemical changes in inhibitory interneurons in specific regions of the hippocampal formation. *Exp Neurol.* 2004; 187:367–379. [PubMed: 15144863]
- Williams S, Vachon P, Lacaille JC. Monosynaptic GABA-mediated inhibitory postsynaptic potentials in CA1 pyramidal cells of hyperexcitable hippocampal slices from kainic acid-treated rats. *Neuroscience.* 1993; 52:541–554. [PubMed: 8095707]

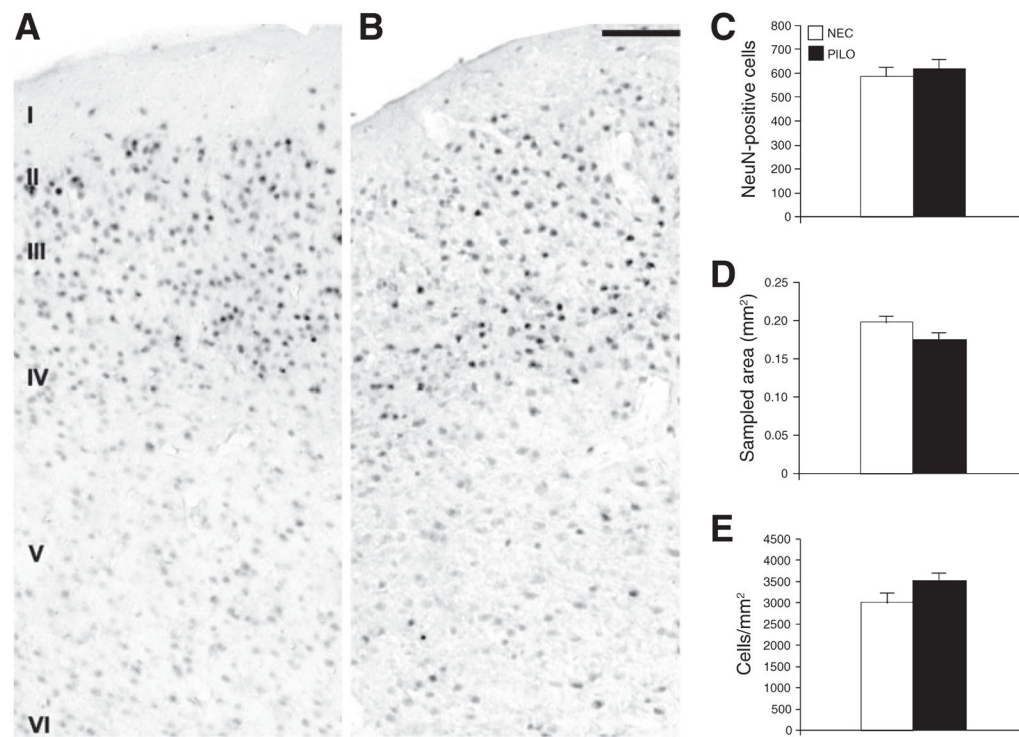


Fig. 1.

Immunohistochemical analysis of neuronal cell distribution in the IC performed with an antibody against NeuN. (A and B) Photomicrographs obtained at approximately 6.38 mm under bregma from NEC and pilocarpine (PILO)-treated rats, respectively. Note that no gross changes in the distribution of NeuN immunoreactivity are visible throughout the various cell layers in the IC of epileptic rats (B) compared with NEC animals (A). Neuronal cell counts (C), sampled areas (D) and densities (E) were not statistically different in NEC (open bars) and PILO-treated (closed bars) rats. Scale bar, 200 μ m.

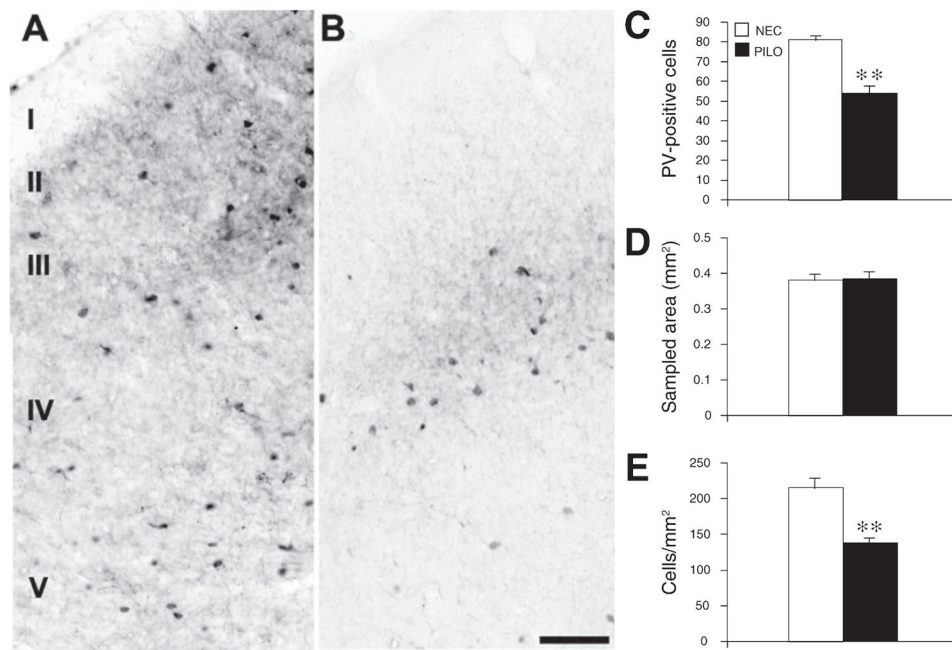


Fig. 2. Immunohistochemical assessment of PV-positive interneurons in the IC. (A and B) Photomicrographs obtained from NEC and pilocarpine (PILO)-treated rats, respectively, at approximately 6.38 mm under bregma. Note that PV-positive cells are decreased in all IC layers after PILO treatment (B) compared with NEC (A). Neuronal cell counts (C) and densities (E) but not the sampled areas (D) were significantly different in NEC (open bars) and PILO-treated (closed bars) rats. ** $P < 0.01$. Scale bar, 200 μm .

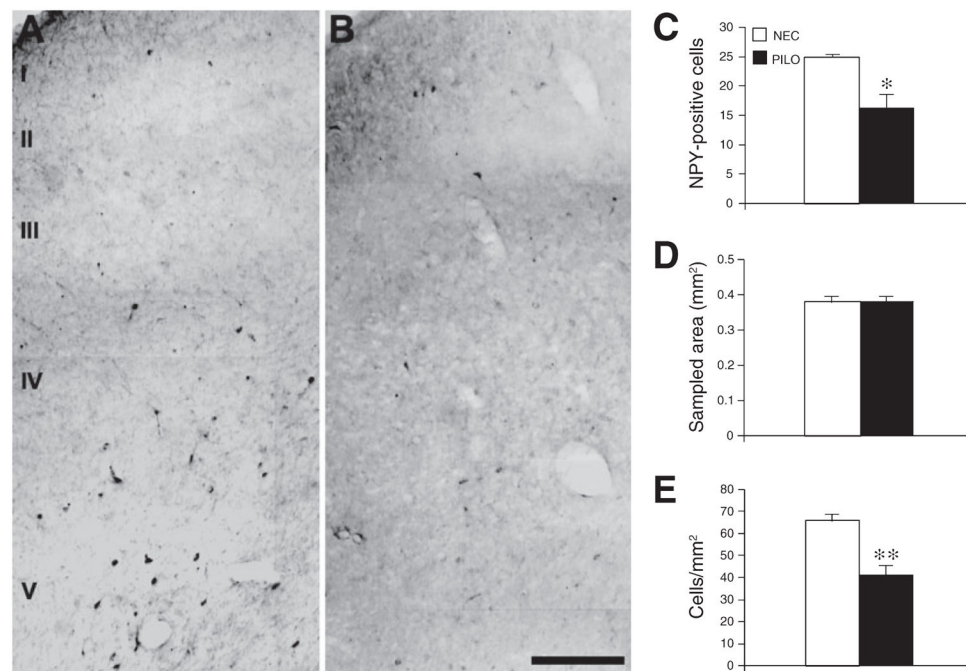
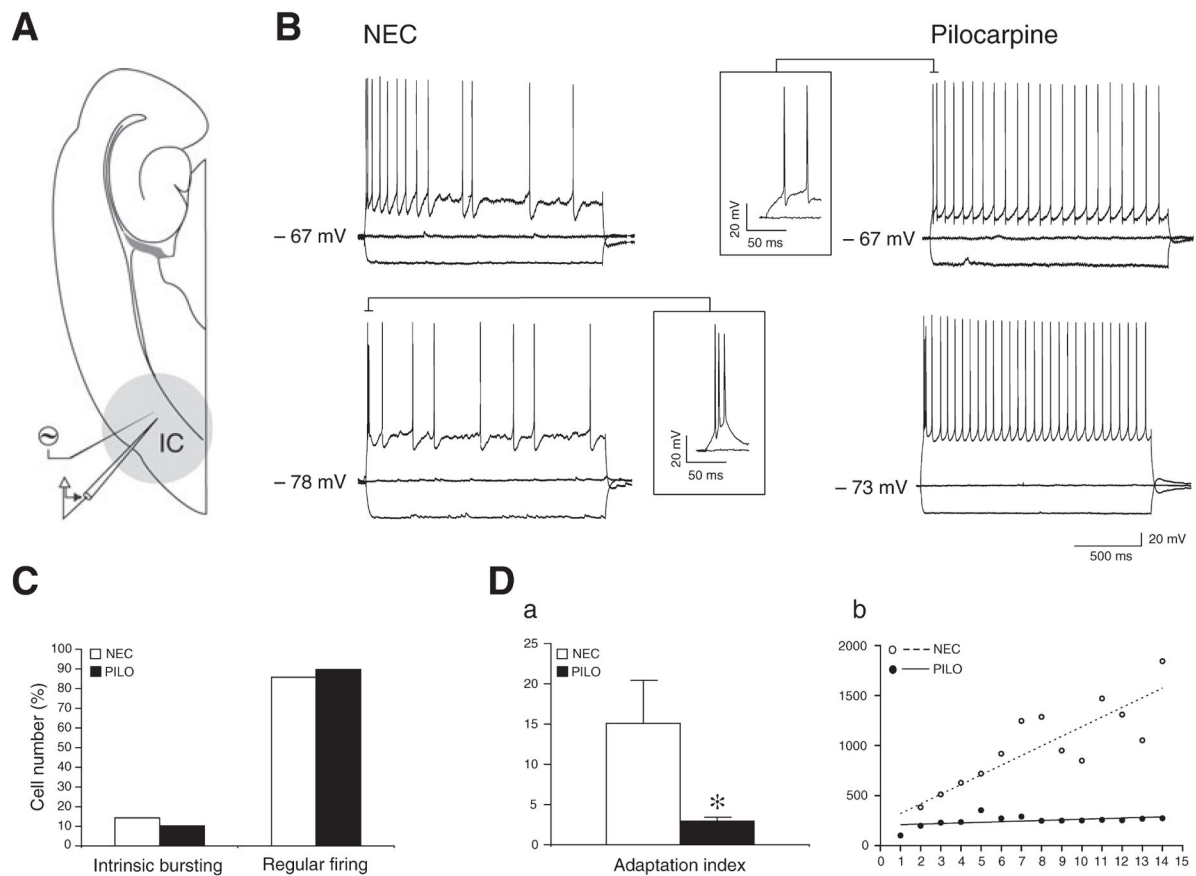
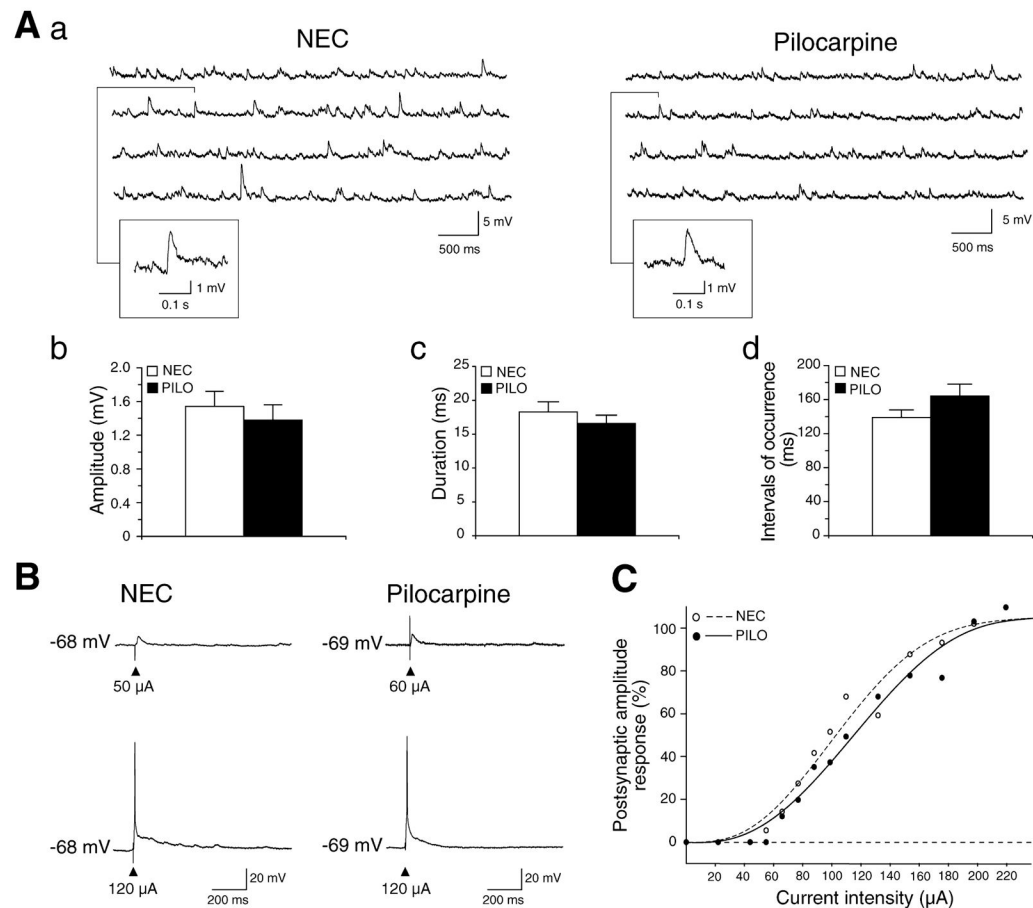


Fig. 3. Immunohistochemical analysis of NPY-positive interneurons in the IC. (A and B) Photomicrographs obtained from NEC and pilocarpine (PILO)-treated rats at approximately 6.38 mm under bregma. Note that NPY-positive cells are decreased in all IC layers in the PILO-treated IC. Note that neuronal cell counts (C) and densities (E) but not the sampled areas (D) were significantly different in NEC (open bars) and PILO-treated (closed bars) rats. * $P < 0.05$, ** $P < 0.01$. Scale bar, 200 μm .

**Fig. 4.**

Repetitive firing properties of IC neurons obtained from NEC and pilocarpine (PILO)-treated rats. (A) Diagram of a typical horizontal combined hippocampus / IC brain slice preparation showing the position of the recording and stimulating electrodes. (B) Two types of firing patterns are generated by IC neurons in NEC and PILO-treated brain slices after the injection of depolarizing current pulses of at least +0.4 nA. (C) Similar percentages of intrinsic bursting and regular firing neurons are seen in the NEC ($n = 24$) and PILO-treated ($n = 25$) IC. (D) (a) Bar graph of the adaptation index of NEC and PILO-treated IC neurons; note that in the latter type of tissue IC neurons are characterized by a smaller value ($*P < 0.05$) when compared with NEC. (b) Linear regression of interevent duration expressed as a percentage of the first measured interval between action potentials in NEC (open circles, $n = 15$) and PILO-treated (black circles, $n = 15$) neurons. Coefficient of determination ($r^2 = 0.6$) for NEC neurons was statistically significant ($P < 0.01$).

**Fig. 5.**

Spontaneous and stimulus-induced synaptic activity generated by NEC and pilocarpine (PILO)-treated IC neurons. (A) Spontaneous postsynaptic potentials recorded at RMP are shown in (a). (b–d) Histograms comparing the amplitude, duration and intervals of occurrence of the postsynaptic potentials recorded in NEC ($n = 10$) and PILO-treated ($n = 10$) cells, respectively. (B) Activation threshold for NEC and PILO-treated IC neurons. (C) Graphical display of the average input / output curves of the postsynaptic responses generated prior to the appearance of action potentials in NEC (open circles, $n = 9$) and PILO-treated (black circles, $n = 9$) cells. Boltzman sigmoidal parameters were used to fit the current–response curves. Stimulus strengths required to evoke half-amplitude responses (NEC: $95.4 \pm 2.6 \mu\text{A}$; PILO: $100.9 \pm 1.9 \mu\text{A}$; $t_{16} = -0.39$, $P = 0.69$) and slopes (NEC: 17.3 ± 2.3 ; PILO: 14.3 ± 1.7 ; $t_{16} = 0.79$, $P = 0.44$) were not statistically significant.

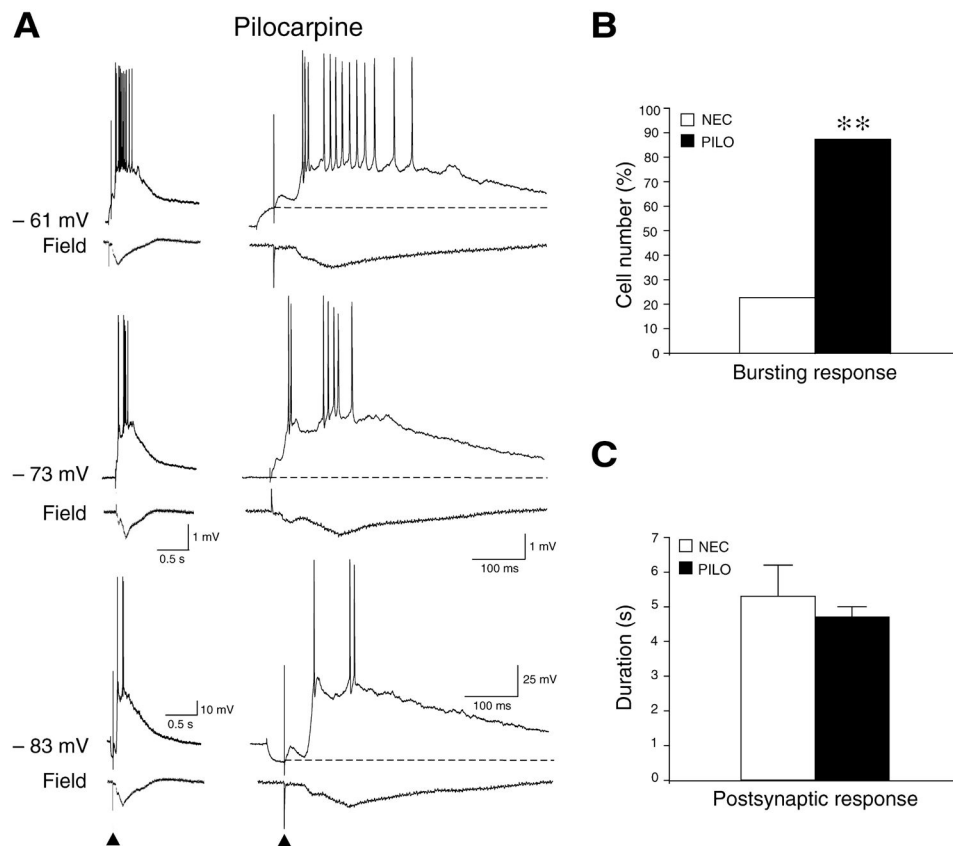
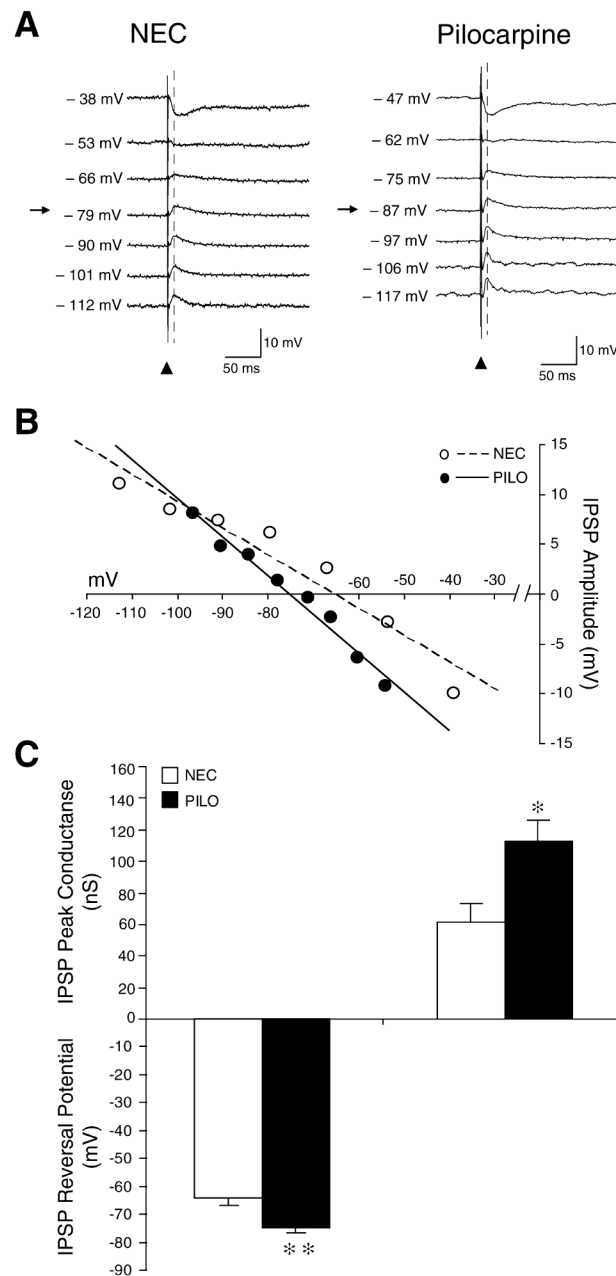


Fig. 6. Single-shock stimulation induces bursting responses in NEC and pilocarpine (PILO)-treated IC neurons. (A) Stimulus-induced, action potential bursting responses recorded in a PILO-treated IC neuron at RMP (–73 mV) and during injection of steady depolarizing current at +0.2 nA (–61 mV) and hyperpolarizing current at –0.2 nA (–83 mV). (B) Bar graph representing the percentage of NEC ($n = 18$) and PILO-treated ($n = 16$) IC cells generating bursting response after the single-shock stimuli. $**P < 0.01$. (C) Bar graph showing the duration of the bursting responses generated by NEC and PILO-treated IC neurons.

**Fig. 7.**

Pharmacologically isolated IPSPs in IC neurons recorded from NEC and pilocarpine (PILO)-treated rats. (A) Representative traces obtained at different membrane potentials from NEC and PILO-treated IC area during single-shock stimuli delivered in the presence of *N*-methyl-D-aspartate (NMDA) and non-NMDA glutamatergic receptor antagonists. Arrows indicate the trace recorded at RMP, whereas triangles represent the stimulus artifacts; the dashed lines identify the time after the stimulus at which measurements were taken. (B) IPSP reversal potentials obtained by measuring the response amplitude induced by focal IC stimulation in an NEC (open circles) and a PILO-treated (black circles) neuron. (C) Histogram representing the reversal potential and peak conductance associated with the

IPSPs recorded in the two types of tissue (NEC = 9 cells; PILO-treated = 12 cells). Note that the reversal potential of IPSPs is more hyperpolarized in PILO-treated IC cells than in NEC as well as that the former type of neurons has a larger peak conductance. * $P < 0.05$, ** $P < 0.01$.

Table 1Intrinsic properties of IC neurons in NEC ($n = 24$) and pilocarpine-treated ($n = 25$) rats

Property	NEC	Pilocarpine
RMP (mV)	-75.91 ± 1.64	-75.88 ± 1.53
Input resistance ($M\Omega$)	44.89 ± 3.85	47.22 ± 3.04
Action potential amplitude (mV)	91.59 ± 2.52	86.98 ± 2.09
Action potential duration (ms)	1.45 ± 0.06	1.47 ± 0.06